

Influence of structural short-range order on the phase diagram of diluted anisotropic Heisenberg ferromagnet

Tadeusz Balcerzak and Karol Szałowski*

Department of Solid State Physics, University of Łódź, ulica Pomorska 149/153, 90-236 Łódź, Poland

(Received 3 July 2009; revised manuscript received 15 September 2009; published 9 October 2009)

The diluted anisotropic Heisenberg ferromagnet is considered in the pair approximation. The structural short-range-order, described by the Warren-Cowley parameter, is taken into account. In the presence of interaction anisotropy, the influence of dilution and structural correlations on the phase diagrams is studied. In particular, for the model in question the critical concentrations and Curie temperatures are calculated for exemplary two-dimensional and three-dimensional lattices.

DOI: [10.1103/PhysRevB.80.144404](https://doi.org/10.1103/PhysRevB.80.144404)

PACS number(s): 75.10.-b, 75.30.-m, 75.50.-y

I. INTRODUCTION

The studies of model diluted magnetic systems have already a long history.¹⁻⁸ Various magnetic systems have been studied, first of all the dilute bulk materials^{1,7,9} but also the ternary alloys¹⁰ and thin films⁸ as well. In these investigations, numerous approximate methods have been employed, the main of which being the molecular-field approximation (MFA),¹⁰ effective-field theory (EFT),^{5,6,9,11,12} Bethe-Peierls-Weiss method,¹ or coherent-potential approximation (CPA).^{3,4} For low-dimensional systems, even some exactly solvable models have been considered.⁷ The dilute alloys have also been the subject of Monte Carlo (MC) simulations,¹³ mainly from the point of view of percolation phenomenon. Using all these methods the critical properties have mostly been studied, for instance, the phase diagrams and critical concentration; however, other magnetic properties (susceptibility, magnetic specific heat, etc.) have also attracted much attention.

In all these classical theoretical works the structural correlations between magnetic atoms have not been taken into account, i.e., a fully stochastic atomic disorder has been assumed. On the other hand, the presence of structural correlations in diluted systems is a well-documented experimental fact.¹⁴ Recently, the importance of the configurational magnetic impurities correlations has been discussed in the models of diluted magnetic semiconductors.^{15,16} For instance, it has been shown in the Ref. 16 how these correlations can be incorporated into the magnetic theory using the so-called Warren-Cowley parameters.¹⁷ It should be stressed that in the paper¹⁶ only the simplest MFA method has been used. It can be argued that the MFA method can be sufficient for the case of the long-range Ruderman-Kittel-Kasuya-Yosida interaction (as considered, for instance, in the Ref. 16) or when the concentration of alloy components is far from the critical concentration (as in Ref. 10). However, for the systems with short-range magnetic interactions and in the presence of strong dilution, the MFA method is inaccurate. Suffice it to mention its inability to predict the nonzero critical concentration.

The simplest method which is superior to MFA and takes into account the spin-pair thermal correlations in a thermodynamically correct manner, is the pair approximation (PA). The advantage of this approach over, for instance, EFT is

such that it enables relatively conveniently to formulate the fully self-consistent thermodynamics. Moreover, the incorporation of configurational pairwise correlations into the PA method, which is intended to be done in this paper, is consistent with this approach.

For the reasons mentioned above, the aim of the present paper is to include the structural short-range-order (SRO) parameter into the magnetic theory which is based on the anisotropic Heisenberg model with the short-range exchange interactions limited to nearest neighbors. The effect of structural correlations, which can either lead to the clustering phenomenon or to the opposite tendency (preference for separation of magnetic atoms), on the magnetic properties will be examined. In particular, the influence of the structural Warren-Cowley parameter on the critical concentration will be studied in the presence of the exchange interaction anisotropy. The phase diagrams will be discussed for the physical range of structural correlations, which is characteristic of a selected crystalline lattice.

The paper is organized as follows: in the next (second) section the theoretical model is developed for the diluted anisotropic Heisenberg ferromagnet, within the PA method with structural correlations taken into account. In Sec. III the numerical results (phase diagrams) will be illustrated in figures and discussed. Then some conclusions from those calculations will be drawn.

II. THEORETICAL MODEL

The model Hamiltonian for a diluted ferromagnetic alloy is assumed in the form of

$$\mathcal{H} = - \sum_{\langle i,j \rangle} [J' (S_i^x S_j^x + S_i^y S_j^y) + JS_i^z S_j^z] \xi_i \xi_j - h \sum_i S_i^z \xi_i, \quad (1)$$

where the external magnetic field h is directed along the z axis and the exchange integrals $0 \leq J' \leq J$ with different J' yield the interaction anisotropy. By changing J' , for one limiting case ($J'=0$) we deal with the diluted pure Ising model whereas for another limit ($J'=J$) the isotropic diluted Heisenberg model is obtained. The spin operators $S_i^\alpha (\alpha=x, y, z)$ for $S=1/2$ are represented by the Pauli matrices. The occupation operators $\xi_i=0, 1$ describe site dilution whereas their configurational average $\langle \xi_i \rangle_r = p$ yields the concentration of magnetic atoms.

In order to take into account the thermal correlations of spin pairs, the PA method¹⁸ will be adopted. This method allows for the Gibbs free-energy calculation and hence the self-consistent thermodynamic description of a magnet can be obtained. The application of the PA method in the formulation described in the Ref. 18 is quite straightforward for the diluted alloy case, when the thermal $\langle \cdots \rangle_T$ and configurational $\langle \cdots \rangle_r$, averaging of operators is performed according to the decoupling scheme,

$$\langle \langle S_i^\alpha S_j^\alpha \xi_i \xi_j \rangle_T \rangle_r = \langle \langle S_i^\alpha S_j^\alpha \rangle_T \xi_i \xi_j \rangle_r \approx \langle S_i^\alpha S_j^\alpha \rangle \langle \xi_i \xi_j \rangle_r. \quad (2)$$

The correlation $\langle S_i^\alpha S_j^\alpha \rangle$ in Eq. (2) is the so-called conditional thermal average, i.e., the average performed under the assumption that i and j sites are occupied. We have also assumed that the occupation operators ξ_i are not subject to thermal averaging, which means that the atomic disorder in the system is of quenched type. The approximation [Eq. (2)] can also be used for the single-site averaging, which yields in this case the result

$$\langle \langle S_i^\alpha \xi_i \rangle_T \rangle_r = \langle \langle S_i^\alpha \rangle_T \xi_i \rangle_r \approx \langle S_i^\alpha \rangle \langle \xi_i \rangle_r, \quad (3)$$

where $\langle S_i^\alpha \rangle$ (the magnetization) is the conditional thermal average.

The above scheme of thermal and configurational averaging can be used not only for Hamiltonian (1), which leads in this case to the mean enthalpy of the system $\langle \langle \mathcal{H} \rangle_T \rangle_r$ but also for the mean entropy $\langle \sigma \rangle_r$, as well. For instance, within the cumulant expansion technique as presented in the Refs. 19 and 20 the mean entropy can be extended here for the diluted alloy case. It takes the form of the following series:

$$\langle \sigma \rangle_r = \sum_i \langle \tilde{\sigma}_i \xi_i \rangle_r + \sum_{(i,j)} \langle \tilde{\sigma}_{ij} \xi_i \xi_j \rangle_r + \cdots, \quad (4)$$

where $\tilde{\sigma}_i$ and $\tilde{\sigma}_{ij}$ are the local single-site and pair entropy cumulants, respectively. Using the approximation analogous to Eqs. (2) and (3), we obtain in the PA method,

$$\langle \sigma \rangle_r \approx Np\sigma_1 + \frac{Nz}{2} \langle \xi_i \xi_j \rangle_r (\sigma_2 - 2\sigma_1), \quad (5)$$

where σ_1 and σ_2 are the conditional single-site and pair entropies, respectively. They can be calculated from the corresponding density matrices of the single-atom and pair clusters embedded in an effective molecular field. Namely,

$$\sigma_1 = -k_B \text{Tr}_i(\rho_i \ln \rho_i) \quad (6)$$

and

$$\sigma_2 = -k_B \text{Tr}_{ij}(\rho_{ij} \ln \rho_{ij}), \quad (7)$$

where ρ_i and ρ_{ij} are the single-site and pair density matrices, respectively. For the occupied sites i, j these matrices can be presented in the form of

$$\rho_i = \frac{\exp[\beta(\Lambda + h)S_i^z]}{2 \cosh\left[\frac{1}{2}\beta(\Lambda + h)\right]} \quad (8)$$

and

$$\rho_{ij} = \frac{\exp\{\beta[J'(S_i^x S_j^x + S_i^y S_j^y) + JS_i^z S_j^z + (\Lambda' + h)(S_i^z + S_j^z)]\}}{2 \left[e^{\beta J'/4} \cosh[\beta(\Lambda' + h)] + e^{-\beta J'/4} \cosh\left(\frac{1}{2}\beta J'\right) \right]}, \quad (9)$$

where Λ and Λ' are the effective molecular fields acting on the single-atom and pair clusters, respectively. N in Eq. (5) is the total number of lattice sites and z is the number of nearest neighbors (NN), i.e., the number of lattice sites on the first coordination zone, being characteristic of a given crystalline lattice.

The structural correlations between the magnetic atoms are conveniently taken into account via the SRO Warren-Cowley parameter α , which is defined by¹⁶

$$\alpha = \frac{\langle \xi_i \xi_j \rangle_r - \langle \xi_i \rangle_r \langle \xi_j \rangle_r}{\langle \xi_i \rangle_r \langle \xi_j \rangle_r}. \quad (10)$$

The particular case with $\alpha=0$ corresponds to the fully stochastic disorder. Hence, the NN occupation correlations are expressed as

$$\langle \xi_i \xi_j \rangle_r = p^2(1 + \alpha). \quad (11)$$

The configurational average of the Gibbs free energy for the diluted alloy can be obtained from the general expression

$$\langle G \rangle_r = \langle \langle \mathcal{H} \rangle_T \rangle_r - T \langle \sigma \rangle_r. \quad (12)$$

Combining the method presented in the Ref. 18 with the decoupling scheme for the occupation operators given above, the mean Gibbs free energy per one lattice site can be finally presented in the form of

$$\frac{\langle G \rangle_r}{N} = \frac{zp^2(1 + \alpha)}{2} \left[G_2 - 2 \frac{zp(1 + \alpha) - 1}{zp(1 + \alpha)} G_1 \right], \quad (13)$$

where

$$G_1 = -k_B T \ln \left\{ 2 \cosh \left[\frac{\beta(\Lambda + h)}{2} \right] \right\} \quad (14)$$

and

$$G_2 = -k_B T \ln \left\{ 2e^{\beta J'/4} \cosh[\beta(\Lambda' + h)] + 2e^{-\beta J'/4} \cosh\left(\frac{\beta J'}{2}\right) \right\}. \quad (15)$$

The molecular fields Λ and Λ' acting on the single spin and the spin belonging to a pair, respectively, are then given by the expressions

$$\Lambda = zp(1 + \alpha)\lambda \quad \text{and} \quad \Lambda' = [zp(1 + \alpha) - 1]\lambda. \quad (16)$$

The variational parameter λ can be determined from the equilibrium condition

$$\frac{\partial \langle G \rangle_r}{\partial \lambda} = 0 \quad (17)$$

which leads to the equation

$$\tanh\left[\frac{\beta(\Lambda + h)}{2}\right] = \frac{\sinh[\beta(\Lambda' + h)]}{\cosh[\beta(\Lambda' + h)] + e^{-\beta J/2} \cosh\left(\frac{\beta J'}{2}\right)}. \quad (18)$$

In order to determine λ , Eq. (18) has to be solved numerically. Relationship (13) for the Gibbs free energy of the diluted alloy is a generalization of the corresponding formula obtained previously for the crystal.¹⁸ In particular, for $p=1$ and $\alpha=0$ we obtain the former result for the crystalline case.

Having obtained the Gibbs free energy [Eq. (13)] all the thermodynamic quantities for the diluted alloy can be calculated whereas the structural correlations are taken into account via the SRO parameter α . In particular, the phase transition (Curie) temperature T_C can be obtained from the linearization of the self-consistent Eq. (18). By setting $\lambda \rightarrow 0$ one gets the formula

$$\exp\left(\frac{J}{2k_B T_C}\right) = \frac{zp(1+\alpha)}{zp(1+\alpha)-2} \cosh\left(\frac{J'}{2k_B T_C}\right). \quad (19)$$

Hence, for the pure Ising model ($J'=0$) we obtain

$$\frac{k_B T_C}{J} = \frac{1}{2 \ln\{zp(1+\alpha)/[zp(1+\alpha)-2]\}}, \quad (20)$$

whereas for the isotropic Heisenberg model ($J=J'$) the result is

$$\frac{k_B T_C}{J} = \frac{1}{\ln\{zp(1+\alpha)/[zp(1+\alpha)-4]\}}. \quad (21)$$

In turn, from the requirement that $T_C \rightarrow 0$ the critical concentration p_c for the diluted alloy can be found. For the case $J' < J$, including the pure Ising model, we obtain

$$p_c = \frac{2}{z(1+\alpha)} \quad (22)$$

and for the isotropic Heisenberg model $J'=J$ the critical concentration is

$$p_c = \frac{4}{z(1+\alpha)}. \quad (23)$$

In general, the temperature phase diagram (for the continuous phase transitions) is described by the Eq. (19), which can be solved numerically. In this equation, the exchange anisotropy of arbitrary value $0 \leq J' \leq J$, the magnetic atom concentration $0 \leq p \leq 1$ and SRO parameter α are taken into account. The estimation of the physical range of the α parameter presents a separate problem which has been extensively discussed in the appendix of the Ref. 16. It can be concluded from the Ref. 16 that in the lowest approximation, when only two first coordination zones are influenced by SRO, the α parameter for the first coordination zone has to fulfil the following 12 inequalities:

$$\begin{aligned} -1 + 2/p - 1/p^2 &\leq \alpha \leq -1 + 2/p, \\ -1 + 1/p - 1/p^2 &\leq \alpha \leq -1 + 1/p, \end{aligned}$$

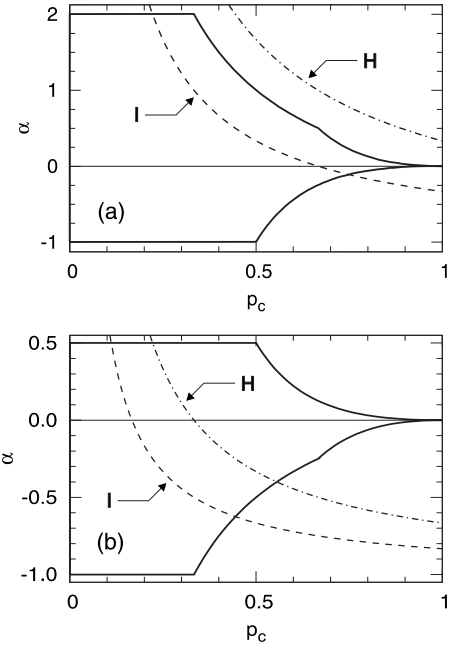


FIG. 1. The critical concentration as a function of Warren-Cowley parameter for nearest neighbors, (a) for 2D honeycomb lattice and (b) for 3D fcc lattice. The bold solid line encloses the physically allowed range of variables. The dashed line (H) is for isotropic Heisenberg case whereas the dashed-dotted one (I) is for anisotropic case.

$$-1 \leq \alpha \leq -1 + 1/p^2,$$

$$\frac{z_2}{z}(1-2/p) \leq \alpha \leq \frac{z_2}{z}(1-2/p+1/p^2),$$

$$\frac{z_2}{z}(1-1/p) \leq \alpha \leq \frac{z_2}{z}(1-1/p+1/p^2),$$

$$\frac{z_2}{z}(1-1/p^2) \leq \alpha \leq \frac{z_2}{z}. \quad (24)$$

where z_2 is the number of lattice sites on the second coordination zone (next-nearest neighbors). Thus, the acceptable limitations on α result not only from the atomic dilution but also from the lattice symmetry. The representative numerical results will be presented in the next section.

III. NUMERICAL RESULTS AND DISCUSSION

The presentation of the numerical results will essentially concern two kinds of lattices: the two-dimensional (2D) honeycomb, which possesses the smallest possible number of NN among the 2D lattices ($z=3$), and the three-dimensional (3D) fcc lattice with the largest coordination number ($z=12$).

Based on the theory presented in the previous section, first of all the critical concentration p_c has been determined vs SRO parameter α . The results are presented in Fig. 1 for the honeycomb [Fig. 1(a)] and fcc [Fig. 1(b)] lattices. Two ex-

TABLE I. Critical concentrations for different lattices without SRO ($\alpha=0$) calculated for the Ising [Eq. (22)] and Heisenberg [Eq. (23)] models and compared with the numerical estimates for the percolation thresholds (Refs. 7 and 13).

z	Ising	Heisenberg	Percolation
2	1		1
3	0.667		0.698 (honeycomb)
4	0.5	1	0.593 (square)
6	0.333	0.667	0.5 (triangular) 0.311 (sc)
8	0.25	0.5	0.245 (bcc)
12	0.167	0.333	0.198 (fcc)

trime cases have been compared in Fig. 1, namely, the isotropic Heisenberg model (H) and the anisotropic Ising-type case for $J' < J$ (I). On account of the limited area of physically allowed α parameter [which has been outlined by the bold borderline in Figs. 1(a) and 1(b)], it is seen that the range of possible concentrations has also been restricted. In particular, it is shown in Fig. 1(a) that the isotropic Heisenberg model on the honeycomb lattice has the critical concentration outside the allowed range for all values of α . Therefore, the occurrence of spontaneous magnetization cannot be expected in that case. It can be mentioned that this result is in agreement with the Mermin-Wagner theorem²¹ for 2D systems without interaction anisotropy. In turn, the Ising model for honeycomb lattice reveals the ferromagnetic order, being mainly apparent for positive α , i.e., when the clustering phenomenon takes place. On the other hand, for fcc lattice the differences between the Ising and Heisenberg models are less pronounced and both models can exhibit the critical concentrations for positive as well as negative α .

It is noteworthy that the critical concentration for the Ising and Heisenberg models is different for all parameters α . Such a difference is obviously expected for 2D systems since the crystalline isotropic Heisenberg model (with $p=1$) does not exhibit magnetic ordering at any nonzero temperature. As mentioned above, this is in accordance with the rigorous Mermin-Wagner theorem.²¹ On the other hand, the crystalline 2D Ising model shows the nonzero phase-transition temperature, which in turn, results from the exact Onsager solution.²² Hence the diluted Ising model should have the critical concentration which is for $p < 1$. However, it should be noted that there exist some works arguing that the critical concentrations of the Ising and Heisenberg models should be the same.²³

In the present method, when the diluted and fully disordered system is concerned (for $\alpha=0$) the critical concentration of the Heisenberg model amounts to $p_c=4/z$ and is twice as big as for the Ising model, where $p_c=2/z$. The value of $p_c=2/z$ for the Ising model without any structural correlations is in agreement with the CPA method^{3,4} and is close to the MC simulations^{7,13} for percolation threshold. The comparison of the results for various lattices is given in Table I. On the other hand, in Fig. 1 it is seen a general tendency that the clustering ($\alpha > 0$) decreases the critical concentration whereas the opposite tendency, favoring sepa-

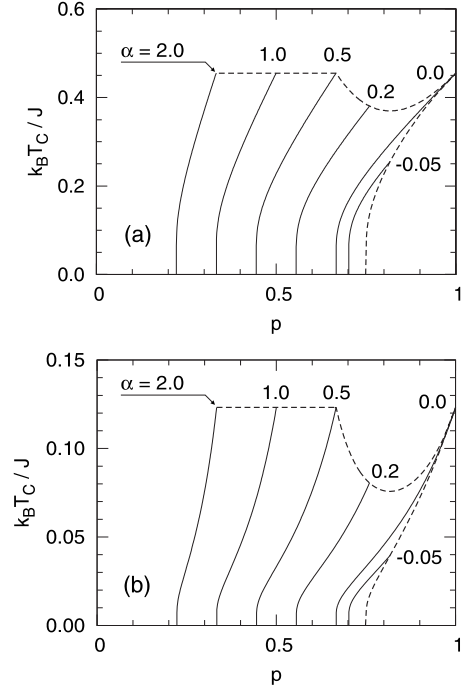


FIG. 2. The critical temperature for honeycomb lattice as dependent on the concentration of magnetic atoms, (a) for pure Ising model and (b) for interaction anisotropy $J'/J=0.9$. Various values of Warren-Cowley parameter were adopted.

ration of magnetic atoms ($\alpha < 0$), increases this value.

In Fig. 2 the critical temperature for the honeycomb lattice is shown vs concentrations of magnetic atoms for the pure Ising model [Fig. 2(a)] and in the presence of anisotropy $J'/J=0.9$ [Fig. 2(b)]. The different curves correspond to the respective SRO parameters α . With the dashed curve the envelope of all those curves is shown, which corresponds to the allowed region of α from Fig. 1. It can be noted that the clustering ($\alpha > 0$) results in a remarkable shift of the phase boundaries with respect to the fully disordered system ($\alpha=0$).

In turn, for the fcc lattice the critical temperature vs concentration is shown in Fig. 3 for the pure Ising model [Fig. 3(a)] and for the isotropic Heisenberg one [Fig. 3(b)]. It is seen in Fig. 3 that the curves corresponding to different α parameters, both positive and negative, are distributed more symmetrically around $\alpha=0$ than in Fig. 2. In both Figs. 2 and 3 the dilution causes decrease in the phase-transition temperature, which eventually vanishes at the critical concentration p_c being characteristic of a given SRO parameter α .

On the basis of the Eqs. (19)–(23), it can be shown that in the vicinity of the critical concentration the Curie temperature for the system depends on p in the following manner:

$$\frac{k_B T_C}{J} = -\frac{1}{2} \left(1 - \frac{J'}{J} \right) \frac{1}{\ln(p - p_c)}, \quad (25)$$

in the presence of anisotropic interaction, i.e., for $J' < J$. Analogously, for the isotropic Heisenberg magnet ($J'=J$) the Curie temperature for $p \rightarrow p_c$ is expressed by

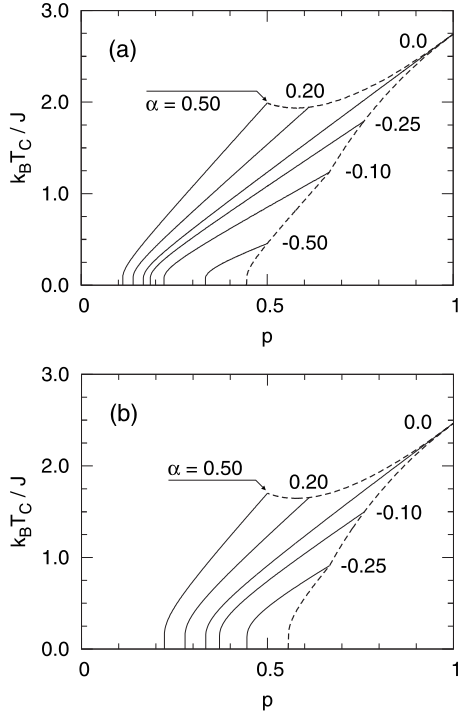


FIG. 3. The critical temperature for fcc lattice as dependent on the concentration of magnetic atoms, (a) for pure Ising model and (b) for isotropic Heisenberg model. Various values of Warren-Cowley parameter were adopted.

$$\frac{k_B T_C}{J} = -\frac{1}{\ln(p - p_c)}. \quad (26)$$

Such a steep, logarithmic dependence of T_C vs p is visible in Figs. 2–4. Let us note that this result is in agreement with the exact behavior expected for diluted ferromagnets near percolation transition, as shown in the Ref. 24 and 25.

The decrease in phase-transition temperature vs concentration is further presented in Fig. 4 for various anisotropy parameters J'/J . Figure 4(a) is prepared for the honeycomb lattice and SRO parameter $\alpha=0.5$ while Fig. 4(b) is for the fcc lattice and $\alpha=-0.25$. It can be concluded from that figure that the existence of anisotropy ($J' < J$) results in distinct increase in the critical temperature. At the same time, it is worth stressing that for the honeycomb lattice we deal with a single critical concentration for all J' (which is the same as for the Ising model) whereas for the fcc lattice two values of critical concentrations have been found. One critical concentration corresponds to the isotropic Heisenberg model ($J' = J$) whereas the other one is for the anisotropic ($J' < J$) case. It is demonstrated in Fig. 4(b) that even introducing minor anisotropy the phase-transition curves rapidly change.

In Fig. 5 the phase diagrams $k_B T_C/J$ vs anisotropy J'/J are presented. Figure 5(a) corresponds to the honeycomb lattice with fixed concentration $p=2/3$ whereas Fig. 5(b) is for the fcc lattice with $p=1/3$. The different curves represent the various SRO parameters α . It is seen that diminishing of anisotropy ($J'/J \rightarrow 1$) results in decrease in the critical temperatures for all α parameters. The critical temperature values $k_B T_C/J$ for the isotropic model ($J' = J$) can either be zero,

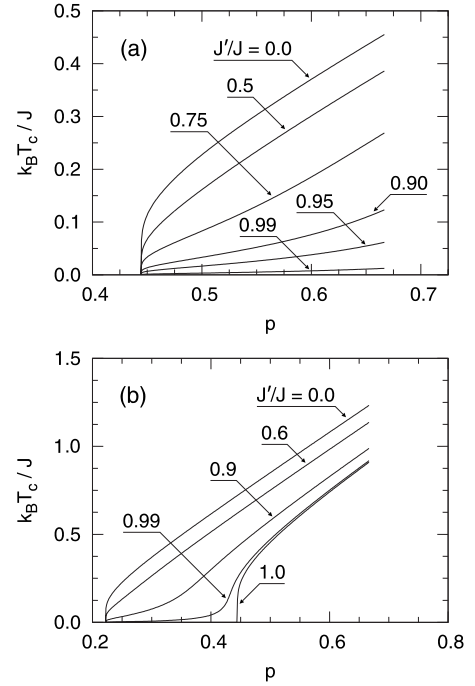


FIG. 4. The critical temperature as a function of concentration of magnetic atoms for various interaction anisotropies, (a) for honeycomb lattice with $\alpha=0.5$ and (b) for fcc lattice with $\alpha=-0.25$.

for $z_{\text{eff}} \leq 4$ or nonzero (for $z_{\text{eff}} > 4$). By $z_{\text{eff}} = zp(1 + \alpha)$ we define the effective number of NN for the given dilution p and SRO parameter α . The curves corresponding to the specific case $z_{\text{eff}}=4$ in Figs. 5(a) and 5(b) have been plotted with a bold line.

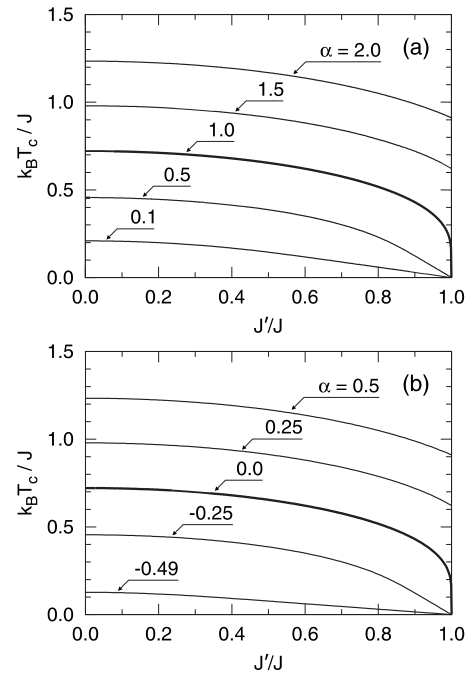


FIG. 5. The critical temperature as dependent on interaction anisotropy for various values of Warren-Cowley parameter, (a) for honeycomb lattice with $p=2/3$ and (b) for fcc lattice with $p=1/3$.

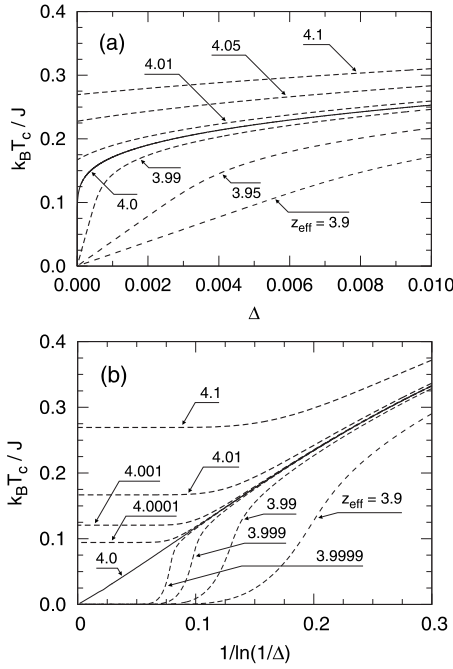


FIG. 6. The critical temperature as dependent on the interaction anisotropy, presented in (a) linear scale and (b) logarithmic scale, in the vicinity of the critical effective coordination number $z_{\text{eff}}=4$ (for which the solid line was plotted).

In order to inspect in more detail the vanishing of critical temperature when $J' \rightarrow J$ and $z_{\text{eff}} \rightarrow 4$, the additional numerical calculations are presented in Fig. 6. For this purpose the new anisotropy parameter $\Delta = (J - J')/J$ has been introduced, which for $\Delta \rightarrow 0$ corresponds to the isotropic Heisenberg model whereas in the limit $\Delta \rightarrow 1$ the pure Ising case is recovered. In Fig. 6 the $k_B T_C/J$ vs Δ [Fig. 6(a)] and $\ln^{-1}(\Delta^{-1})$ [Fig. 6(b)] is presented when z_{eff} is from the range $3.9 \leq z_{\text{eff}} \leq 4.1$. It can be seen that $z_{\text{eff}}=4$ is the critical effective number of NN, below which the Heisenberg model (for $\Delta = 0$) is magnetically disordered at any temperature. The vanishing of T_C for $\Delta \rightarrow 0$ and $z_{\text{eff}}=4$ is much slower than linear, as it is seen in Fig. 6(a). However, in the coordinates chosen for Fig. 6(b) the decrease becomes linear vs $\ln^{-1}(\Delta^{-1})$ and we have found that in the PA method its slope coefficient is equal to unity.

The linear dependency shown in Fig. 6(b) can be substantiated on the basis of Eq. (19) when $z_{\text{eff}} = zp(1 + \alpha) = 4$. Then we get

$$\exp(\beta_C J/2) = \exp(\beta_C J'/2) + \exp(-\beta_C J'/2). \quad (27)$$

Substituting $J' = J(1 - \Delta)$ into Eq. (27) and making use of the linear expansion $\exp(\pm \beta_C J \Delta/2) \approx 1 \pm \beta_C J \Delta/2$, which is valid for $\beta_C J \Delta \rightarrow 0$, we obtain

$$\beta_C J \Delta/2 = \exp(-\beta_C J)(1 + \beta_C J \Delta/2), \quad (28)$$

hence for $\Delta \rightarrow 0$

$$\beta_C J = \ln\left(1 + \frac{2}{\beta_C J \Delta}\right) \approx \ln\left(\frac{2}{\beta_C J \Delta}\right). \quad (29)$$

Equation (29) can be written in the equivalent form

$$\left(\frac{k_B T_C}{J}\right) \left[\ln\left(\frac{2k_B T_C}{J}\right) + \ln\left(\frac{1}{\Delta}\right) \right] = 1. \quad (30)$$

Now, one can make use of the limit $x \ln(2x) \rightarrow 0$ for $x \rightarrow 0$. Thus, from Eq. (30) we obtain the final formula

$$\frac{k_B T_C}{J} = \frac{1}{\ln(1/\Delta)} \quad (31)$$

valid for $\Delta \rightarrow 0$ and $z_{\text{eff}}=4$. The relationship (31), obtained here in the PA method, is in qualitative agreement with the mean-field renormalization group approach and considerations presented in the Refs. 26 and 27, as well as with the Monte Carlo simulations^{28,29} and even with some rigorous estimations.³⁰

In a similar way, we have found from Eq. (19) that for $2 < z_{\text{eff}} < 4$ the critical temperature dependence on Δ is linear when $\Delta \rightarrow 0$ and reads

$$\frac{k_B T_C}{J} = \frac{1}{2 \ln\{z_{\text{eff}}/[2(z_{\text{eff}} - 2)]\}} \Delta. \quad (32)$$

Such a linear dependency is in agreement with Fig. 6(a). Moreover, for $z_{\text{eff}} > 4$ the expression for T_C is also linear vs Δ (for $\Delta \rightarrow 0$) and is of the form

$$\frac{k_B T_C}{J} = \frac{1}{\ln[z_{\text{eff}}/(z_{\text{eff}} - 4)]} \left(1 + \frac{2}{z_{\text{eff}} - 4} \Delta\right). \quad (33)$$

In particular, when $\Delta=0$ we obtain from Eq. (33) the Curie temperature of isotropic Heisenberg model given by Eq. (21).

IV. CONCLUSION

The PA method, recently developed for the anisotropic Heisenberg model,¹⁸ has been extended here for the diluted alloy case with the SRO parameter taken into account. In particular, the phase-transition temperatures and the critical concentrations have been calculated. It has been demonstrated that within the PA method, the critical concentrations for the isotropic Heisenberg model are different than for the Ising one [Eqs. (22) and (23)]. It has been found that the SRO parameter has a great influence on the critical temperature of diluted magnet and, in particular, on the critical concentration p_c . The Curie temperature dependencies on the atomic concentration in the vicinity of p_c have been derived for the anisotropic and isotropic models in the form of logarithmic laws [Eqs. (25) and (26), respectively]. The influence of the anisotropy in the presence of dilution has also been studied and some analytical formulas (31)–(33) for the limiting case $\Delta \rightarrow 0$ have been obtained.

As far as the PA method is concerned, the possibility of handling the Gibbs free energy, and hence the self-consistent calculation of all thermodynamic properties as well as its applicability for low-dimensional systems reflects well the usefulness of this approach. At the same time, some deficiencies of the method, which have been discussed in the Ref. 18 for the crystalline systems, remain here and become transferred to the description of the structurally disordered

magnets. A noticeable difficulty arising in the context of PA is connected with undistinguishable lattices which possess the same coordination number z but indicate different symmetry. An example is $z=6$, both for the 3D simple cubic lattice and 2D triangular one. It can be noticed that in the

case of the annealed limit the star-triangle transformation might be helpful³¹ by enabling to transform the triangular lattice into an equivalent honeycomb one. However, for such a case an appropriate reformulation of the PA method would be required.

*kszalowski@uni.lodz.pl

- ¹H. Sato, A. Arrott, and R. Kikuchi, *J. Phys. Chem. Solids* **10**, 19 (1959).
- ²S. H. Charap, *Phys. Rev.* **126**, 1393 (1962).
- ³T. Tahir-Kheli, *Phys. Rev. B* **6**, 2808 (1972).
- ⁴T. Oguchi, I. Ono, and T. Ishikawa, *J. Phys. Soc. Jpn.* **35**, 1586 (1973).
- ⁵N. Matsudaira, *J. Phys. Soc. Jpn.* **35**, 1593 (1973).
- ⁶T. Kaneyoshi, I. P. Fittipaldi, and H. Beyer, *Phys. Status Solidi B* **102**, 393 (1980).
- ⁷R. B. Stinchcombe, in *Phase Transitions and Critical Phenomena*, edited by C. Domb and M. S. Green (Academic, London, 1983), Vol. 7, pp. 152–281.
- ⁸T. Balcerzak, J. Mielnicki, G. Wiatrowski, and A. Urbaniak-Kucharczyk, *J. Phys.: Condens. Matter* **2**, 3955 (1990).
- ⁹T. Kaneyoshi and M. Jaščur, *Phys. Status Solidi B* **173**, K37 (1992).
- ¹⁰J. Dely and A. Bobák, *J. Magn. Magn. Mater.* **305**, 464 (2006).
- ¹¹N. Benayad, A. Benyoussef, and N. Boccara, *J. Phys. C* **18**, 1899 (1985).
- ¹²M. Kerouad, M. Saber, J. W. Tucker, *Phys. Status Solidi B* **180**, K23 (1993).
- ¹³D. Stauffer, *Phys. Rep.* **54**, 1 (1979).
- ¹⁴J. M. Cowley, *J. Appl. Phys.* **21**, 24 (1950).
- ¹⁵G. Bouzerar, T. Ziman, and J. Kurdnowský, *Appl. Phys. Lett.* **85**, 4941 (2004).
- ¹⁶K. Szałowski and T. Balcerzak, *Phys. Rev. B* **77**, 115204 (2008).
- ¹⁷J. M. Cowley, *Phys. Rev.* **77**, 669 (1950).
- ¹⁸T. Balcerzak and I. Łuźniak, *Physica A* **388**, 357 (2009).
- ¹⁹D. J. Bukman, G. An, and J. M. J. van Leeuwen, *Phys. Rev. B* **43**, 13352 (1991).
- ²⁰T. Balcerzak, *Physica A* **317**, 213 (2003).
- ²¹N. D. Mermin and H. Wagner, *Phys. Rev. Lett.* **17**, 1133 (1966).
- ²²L. Onsager, *Phys. Rev.* **65**, 117 (1944).
- ²³R. J. Elliott, B. R. Heap, D. J. Morgan, and G. S. Rushbrooke, *Phys. Rev. Lett.* **5**, 366 (1960).
- ²⁴S. Sachdev, *Quantum Phase Transitions* (Cambridge University Press, Cambridge, 1999).
- ²⁵D. Stauffer and A. Aharony, *Introduction to Percolation Theory*, 2nd revised ed. (Taylor & Francis, London, 2003).
- ²⁶J. Ricardo de Sousa and I. G. Araújo, *Phys. Lett. A* **272**, 333 (2000).
- ²⁷J. Ricardo de Sousa, N. S. Branco, B. Boechat, and C. Cordeiro, *Physica A* **328**, 167 (2003).
- ²⁸K. Binder and D. P. Landau, *Phys. Rev. B* **13**, 1140 (1976).
- ²⁹P. A. Serena, N. García, and A. Levanyuk, *Phys. Rev. B* **47**, 5027 (1993).
- ³⁰J. Bricmont and J.-R. Fontaine, *Commun. Math. Phys.* **87**, 417 (1982).
- ³¹C. Domb, *Adv. Phys.* **9**, 149 (1960).